Applied Surface Science 258 (2012) 2226–2230

Contents lists available at SciVerse ScienceDirect

Applied Surface Science

journal homepage: www.elsevier.com/locate/apsusc

Structural stability of nano-sized crystals of HMX: A molecular dynamics simulation study

H. Akkbarzade[a,*], G.A. Parsafar[a,b], Y. Bayat[a]

[a] Department of Chemistry, Sabzevar Tarbiat Moallem University, Sabzevar, Iran
[b] Nano-Technology Center, Sharif University of Technology, Azadi Avenue, Tehran, Iran

ARTICLE INFO

Article history:
Received 15 June 2011
Received in revised form 24 August 2011
Accepted 25 August 2011
Available online 3 September 2011

Keywords:
Molecular-dynamics
HMX nanoparticle
Structural stability
Sublimation enthalpy

ABSTRACT

The interaction potential energy and heat of sublimation of nanoparticles of HMX crystal polymorphs are studied by using molecular dynamics methods with a previously developed force field [Bedrov, et al., J. Comput.-Aided Mol. Des. 8 (2001) 77]. Molecular dynamics simulations of nanoparticles with 10, 20, 30, 40, 50, 60, 70, 80, 90, and 100 molecules of HMX are carried out at 300 K. The intermolecular, intramolecular and total interaction energies per mole for the nanoparticles are calculated at 300 K. Then, we have calculated sublimation enthalpy of HMX crystal polymorphs with different sizes. For the all sizes, the β-HMX is found to be the most stable phase, due to having the least total interaction energy. Also, α-HMX is more stable than δ-HMX. An increase in the sublimation enthalpy with the size of the nanoparticle can be seen.

1. Introduction

Very fine particles of materials in fact exhibit properties significantly different from those of the same material with large sizes. In the case of solid explosives and propellants small particles are required to improve the combustion process. Indeed, the maximum energy output from a detonation is related to the particle size of material [1].

Development of energetic materials with improved performance and reduced sensitivity characteristics are major goals in the area of high energy materials (HEMs). Crystal morphology of these materials plays a vital role in the sensitivity aspects. The physical characteristics of a HEM such as crystal size, shape, morphology, purity, internal and external defects and the microstructure of internal crystalline voids play vital roles in sensitivity of HEMs. One of the approach to lower the sensitivity towards mechanical stimuli is to control the crystal size [2,3].

The microstructural properties of an energetic material strongly influence the combustive and explosive behavior of the formulations [4,5]. These differences can be attributed in part to the strong influence of the heat and mass transport rate which are affected by many factors. Among these, the particle size of the energetic materials [6] and the homogeneity of the formulations play the major role.

HMX (octahydro-1,3,5,7-tetranitro-1,3,5,7-tetrazocine) is a high explosive material used in many plastic bonded explosives (PBX), double base propellants and propellant composite because of its high calorific potential, high density and smokeless combustion products [7,8].

Preparation of nanoscale high explosive materials like pentaerythritol tertanitrate (PETN) and cyclotetramethylene tetranitramine (HMX) has been a challenging task, due to their chemical and physical properties such as decomposition at relatively low temperatures. HMX is used almost exclusively in military applications and also as a propellant. It has also been the subject of various fundamental studies [9–12]. Although these materials have extensively been studied at the macroscopic level, very little is known about their behavior at the nanoscale. Engineering and control of energetic material properties at the nanoscale are of paramount important when the ignition and detonation properties of high explosive (HE) are to be determined.

There are four different crystal structures for HMX, three pure crystal phases, α, β and δ, and a hydrated phase γ [13]. At ambient conditions, the relative stabilities of these bulk polymorphs are known to be β > α > γ > δ [14].

In recent years, many studies have been done on the HMX by molecular dynamics simulations.

Smith and Bharadwaj obtained the force field energies and geometries for the low-energy conformers of HMX [15]. Bedrov et al. used a quantum chemistry-based intra- and intermolecular force field to predict the crystal structures, coefficients of thermal expansion, and heat of sublimation for three pure polymorphs of HMX (α, β, δ); and the sound speed of β-HMX at 295 K;

* Corresponding author. Tel.: +98 21 66165355; fax: +98 21 66005718.
E-mail address: akbarzadehhamed@yahoo.com (H. Akkbarzade).

0169-4332/$ – see front matter © 2011 Elsevier B.V. All rights reserved.
doi:10.1016/j.apsusc.2011.08.101

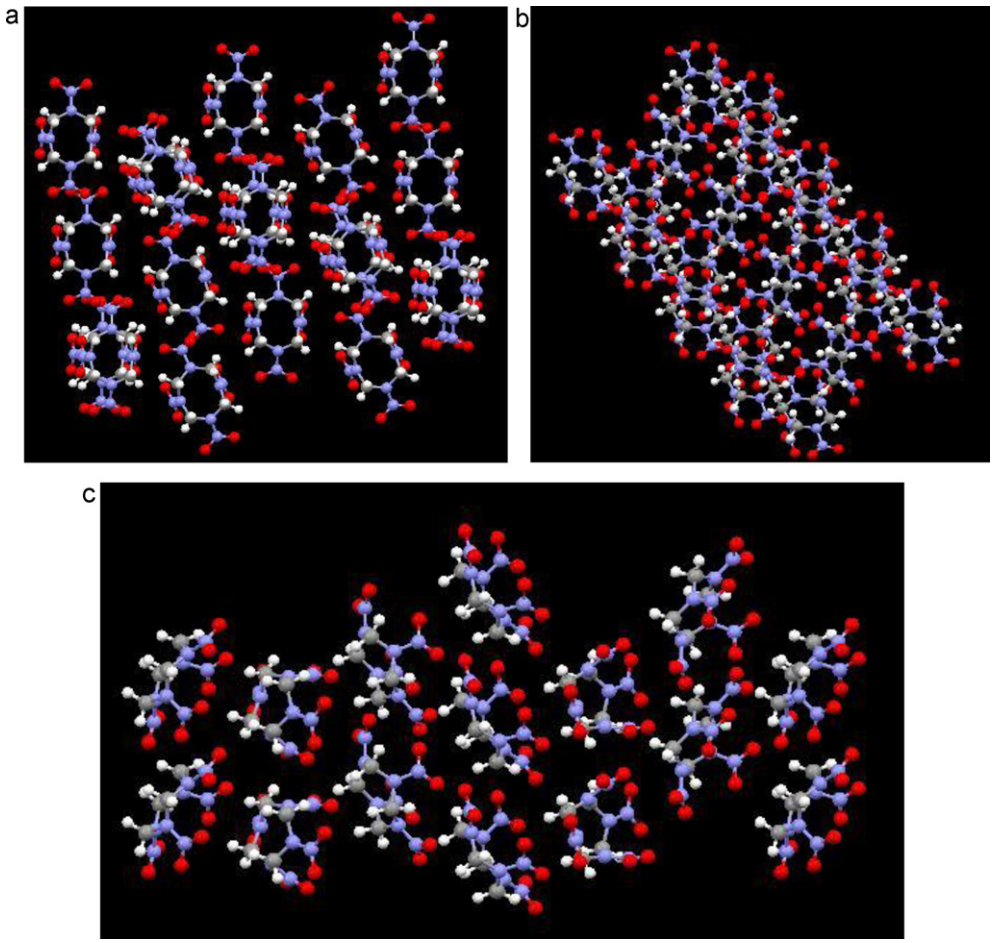

Fig. 1. A snapshot for (a) α, (b) β and (c) δ nano-HMX phases with 20 molecules, respectively.

all at the atmospheric pressure (via molecular dynamics simulations) [16]. Bedrov et al. performed an extensive MD simulation of liquid HMX within the temperature range of 550 K < *T* < 800 K at atmospheric pressure to predict the shear viscosity and molecular self-diffusion coefficient [17]. Sewell et al. predicted the isotherms, isothermal elastic coefficients, and derived isotropic moduli of the three pure polymorphs of HMX at atmospheric pressure and 295 K [18]. Bedrov et al. determined the thermal conductivity of liquid HMX from imposed heat flux non-equilibrium molecular dynamics (NEMD) simulations. The thermal conductivity was determined in the temperature domain of 550 K < *T* < 800 K, which corresponds approximately to the temperature range of the liquid phase of HMX at atmospheric pressure [19]. Duan et al. investigated the solvent effects on the crystal morphology of HMX [20]. Cui et al. performed MD simulations to study the phase transition and mechanical properties of the energetic materials of α-, β- and δ-HMX. The effect of pressure and temperature on the structures and mechanical properties are discussed [21].

The aim of the present work is to predict the relative stability of pure polymorphs of nano-HMX (α, β, δ) at 300 K and atmospheric pressure for different sizes, via the molecular dynamics simulation. We have selected similar sizes for three phases of HMX (10–100 molecules of HMX).

This paper is organized as follows: Section 2 presents a summary of molecular dynamics simulation trend, including the force field models and simulation details. In Section 3, we have compared potential energy both in bulk and nano-HMX. Also, we have calculated heat of sublimation of the three pure polymorphs of nano-HMX with different sizes (α, β, δ). This is followed by a conclusion in the last section.

2. Molecular dynamics simulations

2.1. Construction of α-, β-, and δ-HMX with different sizes

The α phase of HMX contains eight $C_4H_8N_8O_8$ molecules per unit cell in an orthorhombic lattice with space group *Fdd*2 [22]. The β phase contains two $C_4H_8N_8O_8$ molecules per unit cell in a monoclinic lattice with space group $P2_1/c$ [23]. The δ phase contains six $C_4H_8N_8O_8$ molecules per unit cell in a hexagonal lattice with space group $P6_1$ [24].

In the β-phase lattice, each $C_4H_8N_8O_8$ molecule has a so-called "chair" conformation in which two neighboring NO_2 groups are on one side of the C_4N_4 ring and the two other NO_2 groups on the opposite side of the ring. This conformation gives the molecule a center of inversion. In contrast, each $C_4H_8N_8O_8$ molecule in the α and δ phases has the so-called "boat" conformation in which all four NO_2 groups are on the same side of the ring [25]. So β phase is less polar, and more symmetric, compared to α and δ phases.

We have made the bulk and nano-HMX with different sizes via Mercury 2.3 [26]. We have selected similar sizes for three phases of HMX (α, β, δ) (specifically with 10, 20, 30, 40, 50, 60, 70, 80, 90, and 100 molecules of HMX). A snapshot for three nanoparticles with 20 molecules of HMX (α, β, δ) is shown in Fig. 1(a)–(c), respectively.

Table 1
Intermolecular, intramolecular and total potential energies per mole for given sizes of different phases of HMX (all in are kcal/mol).

N	E_α (intra)	E_δ (intra)	E_δ (intra)	E_α (inter)	E_β (inter)	E_δ (inter)	E_α (total)	E_β (total)	E_δ (total)
10	472.5	466.7	476.0	−21.9	−21.5	−22.1	450.6	445.2	453.9
20	472.7	466.9	476.3	−28.8	−26.8	−29.0	443.9	440.1	447.3
30	472.4	466.4	476.1	−34.0	−32.5	−33.8	438.4	433.9	442.3
40	472.4	466.6	476.0	−39.1	−37.8	−39.4	433.3	428.8	436.6
50	472.6	466.3	476.2	−43.2	−41.1	−43.1	429.4	425.2	433.1
60	472.2	466.8	475.9	−46.5	−43.1	−46.8	425.7	423.7	429.1
70	472.8	466.6	476.2	−48.9	−44.7	−49.0	423.9	421.9	427.2
80	472.5	466.7	476.1	−50.6	−46.0	−50.4	421.9	420.7	425.7
90	472.9	466.6	476.2	−51.9	−46.9	−52.0	421.0	419.7	424.2
100	473.0	466.7	476.15	−52.8	−47.7	−52.6	420.2	419.0	423.5
Bulk	472.9	466.9	476.2	−52.9	−47.8	−52.8	420.0	419.1	423.4

2.2. The force field of HMX

A flexible force field used for HMX was developed by Smith and Bharadwaj [15] some with minor modifications of Bedrov et al. [16]. This force field was developed by using quantum-chemistry calculations. In this paper we shall present results of the MD simulations using the same force field for the three pure crystal polymorphs of HMX.

The intramolecular potential, V_{intra}, has the functional form:

$$V_{\text{intra}} = V_{\text{bond}} + V_{\text{bend}} + V_{\text{torsion}} + V_{\text{inversion}} \quad (1)$$

where V_{bond}, V_{bend}, V_{torsion}, and $V_{\text{inversion}}$ are bonding potential, bending potential, torsional potential and inversion potential, respectively.

The bonding potentials are described by the harmonic functions:

$$V_{\text{bond}} = 0.5k_{\text{b}}(r - r_0)^2 \quad (2)$$

where k_{b} is the force constant and $r - r_0$ is the displacement from the equilibrium position.

The twenty-eight bonding potentials correspond to the O–N (eight), N–N (four), N–C (eight), and C–H (eight) bonds. The bending potentials are described by the harmonic functions as,

$$V_{\text{bend}} = 0.5k_{\text{a}}(\theta - \theta_0)^2 \quad (3)$$

where k_{a} is the force constant and $\theta - \theta_0$ is the angular deviation from the equilibrium value.

The forty-eight bending potentials corresponds to the ONO (four), ONN (eight), NNC (eight), CNC (four), NCH (sixteen), HCH (four), and NCN (four) angles.

The torsional potential is a cosine function:

$$V_{\text{torsion}} = 0.5k_{\text{d}}[1 - \cos(n\varphi)] \quad (4)$$

where k_{d} is the force constant and $n\varphi$ is the dihedral angle.

The eighty-eight torsional potential terms correspond to the $ONNC^1$ (sixteen), $ONNC^2$ (sixteen), $ONNC^3$ (sixteen), HCNC (sixteen), $CNCN^1$ (eight), $CNCN^2$ (eight), and $CNCN^3$ (eight) dihedrals.

Each inversion potential is taken to be harmonic,

$$V_{\text{inversion}} = 0.5k_{\text{i}}\delta^2 \quad (5)$$

where k_{i} is the force constant and δ is the out of plane angle.

The eight inversion potential functions correspond to the CNCN (four) and ONON (four) out of plane bending.

The intermolecular potential is summation of the Buckingham and Coulombic terms:

$$V_{\text{intermolecular}} = \sum_i \sum_j \left[A_{ij}\exp(-Br_{ij}) - \left(\frac{C_{ij}}{r_{ij}^6}\right) + \left(\frac{q_i q_j}{4\pi\varepsilon_0 r_{ij}}\right) \right] \quad (6)$$

where r_{ij} is the interatomic distance between atoms i and j of two different molecules and q_i and q_j are their electrostatic charges. The details regarding the force field parameters are given in references [15,16].

2.3. Simulation protocol

In the present study, molecular-dynamics calculations on bulk and nanoparticles of HMX (for α, β, and δ phases of HMX) were carried out by the DLPOLY 2.18 program [27]. The bulk calculations were done with the *NPT* ensemble at ambient pressure and with the periodic boundary conditions, applying a Nose–Hoover thermostat–barostat [28–30] with the relaxation times for the temperature and pressure of 0.1 and 1.0 fs, respectively. The Verlet leapfrog scheme was used to integrate the equations of motion. The Ewald's method was applied to deal with the long-range electrostatic forces [30,31]. In these calculations, a time step of 1 fs was used and trajectories were carried out for a total of 100 ps, with the first 50 ps used to equilibrate the system.

Simulations of the nanoparticles were done with the *NVE* ensemble with no periodic boundary conditions. A time step of 0.1 fs was used, and the total duration of the nanoparticle simulations was 2 ns, with the first 1 ns used for the equilibration. The electrostatic forces were directly calculated for the finite number of nanoparticles. Ten sets of nanoparticle simulations, specifically with 100, 90, 80, 70, 60, 50, 40, 30, 20, and 10 HMX molecules, were performed for the α, β, and δ HMX phases.

All interatomic interactions were determined for the atoms in the simulation within a cutoff distance of R_{cutoff}. For the largest nanoparticle, the value of R_{cutoff} = 12.0 Å was used. The cutoff distance was appropriately adjusted for the smaller nanoparticles.

3. Results and discussions

In these simulations, we have calculated the intermolecular, intramolecular and total interaction energies per mole for different sizes of solid HMX. The results of obtained potential energy are summarized in Table 1 at 300 K for given sizes of α-, β-, δ-HMX, in which E_{intra}, E_{inter}, and E_{total} are the intramolecular, intermolecular and total potential energies per mole.

As shown in Table 1, the β-phase in both bulk and nanoparticles states has a higher intermolecular potential energy than its corresponding α and δ phases. Owing to the fact that the former molecular conformation is nonpolar such a result is expected, due to the existence of the dipole–dipole interactions among the latter conformations. Therefore, the intermolecular potential energy in the α and δ phases is more negative than that of the β phase.

Also, as shown in Table 1, the β-phase in both bulk and nanoparticles states has a lower intramolecular potential energy than its corresponding α and δ phases. The lower intramolecular potential energy of β phase may be attributed to the following factors: since in the α and δ phases, all four NO_2 groups are on the same side of the ring but in β-phase, two neighboring NO_2 groups are on one side of the C_4N_4 ring and two others on the other side, we may expect that,

Table 2
Intermolecular and intramolecular potential energies per mole for the α, β, and δ-HMX ideal gas (in terms of kcal/mol).

Ideal gas	α-HMX	β-HMX	δ-HMX
E_{inter}	0	0	0
E_{intra}	465.9	466.1	466.3

1. When NO_2 groups with the negative charges are located on one side of the C_4N_4 ring, there would be strong Columbic repulsions among them.
2. Also, when four NO_2 groups are in the same side of the ring, the steric factor becomes more significant.

Both mentioned factors lead to a lower intramolecular potential energy for the β phase, compared to two other phases.

We have also simulated the HMX molecule with same conformations as in the crystal phases, without any interactions among different molecules, i.e. in the ideal gas state. Table 2 shows the E_{inter} and E_{intra} for the ideal gas of the α-, β-, and δ-HMX (in units of kcal/mol).

There is no interaction among molecules of HMX in the ideal gas state; therefore E_{inter} is zero for all phases in their ideal gas states. But, E_{intra} is different for the phases, because the molecular conformations of three phases are different. As shown in Table 2, for the ideal gas state, $E_{intra,\delta} > E_{intra,\beta} > E_{intra,\alpha}$.

The sublimation enthalpy, $\Delta H_{sub,}$ can be simply calculated as,

$$\Delta H_{sub} = H_{gas} - H_{solid} = RT + \Delta E_{inter} + \Delta E_{intra} \quad (7)$$

where R is the universal gas constant, ΔE_{inter} and ΔE_{intra} are the differences in intermolecular and intramolecular potential energies of HMX molecules in the ideal gas and corresponding crystal phases, respectively [16]. The values of ΔE_{inter} and ΔE_{intra} can be calculated by using the data of Tables 1 and 2, for the three phases with any given sizes.

The value of ΔE_{intra} is negative for the bulk and nanosystems of α-, β-, δ-HMX (varies from −7.1 to −6.5 kcal/mol). This means that the internal energy in the ideal gas state is less than its corresponding solids. ΔE_{intra} is independent of system size, but ΔE_{inter} depends on the system size (changes within 26–30 kcal/mol depending on the solid phase). For all three phases, ΔE_{inter} increases with the system size, especially for smaller values of N. Owing to the fact that the bonding energy of a surface molecule is less than that of a molecule inside the bulk, such dependence is reasonable.

Then by having the values of ΔE_{intra} and ΔE_{inter}, Eq. (7) can be used to calculate ΔH_{sub} for the phases with any given sizes.

The calculated values of ΔH_{sub} are given in Table 3 at 300 K for different sizes of α-, β-, and δ-HMX.

As shown In Table 3, for all given sizes β-HMX is more stable than α-HMX, and α-HMX is more stable than δ-HMX. The experimental value for ΔH_{sub} of the bulk HMX is 44.16 and 42.04 kcal/mol for the β and δ phases, respectively [32,33] which are in good agreement with our MD results.

Also, structural stability and sublimation enthalpy are very useful for understanding safety of HMX in different crystal phases. More sublimation enthalpy shows that the system is safer (Since the solid energetic materials convert to small gaseous molecules in an explosion, less sublimation energy means higher heat release, hence stronger explosion is expected. However, the rate of reaction depends on the reaction mechanism.) Therefore, for all given sizes β-HMX is safer than α-HMX, and α-HMX is safer than δ-HMX. In Table 3 an increase in sublimation enthalpy with nanoparticle size can be observed. Therefore, in all three crystalline phases, an increase in safety with nanoparticle size can be observed.

Table 3
The calculated value of ΔH_{sub} of HMX polymorphs from the MD simulations at 300 K (in units of kcal/mol).

N	$\Delta H_{sub}(\alpha)$	$\Delta H_{sub}(\beta)$	$\Delta H_{sub}(\delta)$
10	15.9	21.5	13.0
20	22.6	26.6	19.6
30	28.1	32.8	24.6
40	33.2	37.9	30.3
50	37.1	41.5	33.8
60	40.8	43.0	37.7
70	42.6	44.8	39.6
80	44.6	46.0	41.2
90	45.5	47.0	42.7
100	46.3	47.7	43.3
Bulk	46.5	47.6	43.5

4. Conclusion

In this work the flexible force field is used for the HMX which was originally developed by Smith and Bharadwaj [15] with minor modifications by Bedrov et al. [16]. In this paper, molecular dynamics simulations for three different HMX nanoparticles with 10, 20, 30, 40, 50, 60, 70, 80, 90, and 100 molecules have been carried out at 300 K. Simulations of the nanoparticles were done with the *NVE* ensemble with no periodic boundary conditions.

In Table 1, the calculated molar potential energy for HMX crystal polymorphs nanoparticles is listed for different sizes, obtained by molecular dynamics simulation. For the β-phase of both bulk and nanoparticles the intramolecular potential energy is lower than those for corresponding α and δ phases. The lower intramolecular potential energy of β phase may be attributed to the two factors: The Columbic repulsions and steric factor of NO_2 groups.

Minor difference in intermolecular potential energy is due to the existence of the dipole–dipole interactions among the molecules of α and δ conformations, but there are not such interactions in the β conformation. Therefore, the intermolecular potential energy in the α and δ phases is more negative than that of the β phase.

We have also calculated sublimation enthalpy via Eq. (7). As shown in Table 3, for the all sizes, β-HMX is the most stable phase, and α-HMX is more stable than δ-HMX. Also, an increase in sublimation enthalpy with nanoparticle size can be observed (see Table 3). As shown in Table 3, regardless of the HMX phase, we may conclude that the nanoparticle becomes more stable when its size increases. Since on one hand a surface molecule is more unstable than its corresponding molecule in the bulk, and on the other hand, the fraction of surface molecules decreases with the particle size, the mentioned conclusion seems to be generally true.

References

[1] J. Jung, M. Perrot, Particle design using supercritical fluids: literature and patent survey, J. Supercrit. Fluids 20 (2001) 179.
[2] O.A. Nafday, R. Pitchimani, B.L. Weeks, J. Haaheim, Patterning high explosives at the nanoscale, Propellants Explos. Pyrotech. 31 (2006) 376.
[3] R. Sivabalan, G.M. Gore, U.R. Nair, A. Saikia, S. Venugopalan, B.R. Gandhe, Study on ultrasound assisted precipitation of CL-20 and its effect on morphology and sensitivity, J. Hazard. Mater. 139 (2007) 199.
[4] Z. Yongxu, L. Dabin, L. Chunxu, Preparation and Characterization of Reticular Nano-HMX, Propellants Explos. Pyrotech. 30 (2005) 438.
[5] G. Yang, F. Nie, T. Li, Q. Guo, Z. Qiao, Preparation and characterization of nano-NTO explosive, J. Energ. Mater. 25 (2007) 35.
[6] T.R. Gibbs, A. Popolato, LASL Explosive Property Data, University of California Press, Berkley, CA, USA, 1980.
[7] M. Fathollahi, S.M. Pourmortazavi, S.G. Hosseini, Particle size effects on thermal decomposition of energetic material, J. Energ. Mater. 26 (2008) 52.
[8] G.F.M. Pinheiro, K. Iha, V.L. Lourenco, Influence of the heating rate in the thermal decomposition of HMX, J. Therm. Anal. Calorim. 67 (2002) 445.
[9] T.R. Gibbs, A. Popolato, LASL Explosive Property Data, University of California Press, Berkeley, CA, USA, 1980.
[10] J.C. Lynch, K.F. Myers, J.M. Brannon, J.J. Delfino, Effects of pH and temperature on the aqueous solubility and dissolution rate of 2,4,6-trinitrotoluene

(TNT), hexahydro-1,3,5-trinitro-1,3,5-triazine (RDX), and octahydro-1,3,5,7-tetranitro-1,3,5,7-tetrazocine (HMX), J. Chem. Eng. Data 46 (2001) 1549.
[11] O.A. Nafday, R. Pitchimani, B.L. Weeks, J. Haahein, Patterning high explosives at the nanoscale, Propellants Explos. Pyrotech. 31 (5) (2006) 376.
[12] D.M. Hoffman, R.W. Swansiger, Partial phase behavior of HMX/DMSO solutions, Propellants Explos. Pyrotech. 24 (1999) 301.
[13] H.H. Cady, L.C. Smith, Los Alamos Scientific Laboratory Report LAMS-2652 TID-4500, Los Alamos National Laboratory, Los Alamos, NM, 1961.
[14] F. Goetz, T.B. Brill, J.R. Ferraro, Pressure dependence of the Raman and infrared spectra of.alpha.-,.beta.-,.gamma.-, and.delta.-octahydro-1,3,5,7-tetranitro-1,3,5,7-tetrazocine, J. Phys. Chem. 82 (1978) 1912.
[15] G.D. Smith, R.K. Bharadwaj, Quantum chemistry based force field for simulations of HMX, J. Phys. Chem. B 103 (1999) 3570.
[16] D. Bedrov, C. Ayyagari, G.D. Smith, T.D. Sewell, R. Menikoff, J. Zaug, Molecular dynamics simulations of HMX crystal polymorphs using a flexible molecule force field, J. Comput.-Aided Mol. Des. 8 (2001) 77.
[17] D. Bedrov, G.D. Smith, T.D. Sewell, Temperature-dependent shear viscosity coefficient of octahydro-1,3,5,7-tetranitro-1,3,5,7-tetrazocine (HMX): a molecular dynamics simulation study, J. Chem. Phys. 112 (2000) 7203.
[18] T.D. Sewell, R. Menikoff, D. Bedrov, G.D. Smith, A molecular dynamics simulation study of elastic properties of HMX, J. Chem. Phys. 119 (2003) 7417.
[19] D. Bedrov, G.D. Smith, T.D. Sewell, Thermal conductivity of liquid octahydro-1,3,5,7-tetranitro-1,3,5,7-tetrazocine (HMX) from molecular dynamics simulations, Chem. Phys. Lett. 324 (2000) 64.
[20] X. Duan, C. Wei, Y. Liuc, C. Pei, A molecular dynamics simulation of solvent effects on the crystal morphology of HMX, J. Hazard. Mater. 174 (2010) 175.
[21] H.L. Cui, G.F. Ji, X.R. Chen, Q.M. Zhang, D.Q. Wei, F. Zhao, Phase transitions and mechanical properties of octahydro-1,3,5,7-tetranitro-1,3,5,7-tetrazocine in different crystal phases by molecular dynamics simulation, J. Chem. Eng. Data 55 (2010) 3121.
[22] H.H. Cady, A.C. Larson, D.T. Cromer, The crystal structure of α-HMX and a refinement of the structure of β-HMX, Acta Crystallogr. 16 (1963) 617.
[23] C.S. Choi, H.P. Boutin, A study of the crystal structure of β-cyclotetramethylene tetranitramine by neutron diffraction, Acta Crystallogr. Sect. B 26 (1970) 1235.
[24] R.E. Cobbledick, R.W.H. Small, The crystal structure of the δ-form of 1,3,5,7-tetranitro-1,3,5,7-tetraazacyclooctane (δ-HMX), Acta Crystallogr. Sect. B 30 (1974) 1918.
[25] H.V. Brand, R.L. Rabie, D.J. Funk, I.D. Acosta, P. Pulay, T.K. Lippert, Theoretical and experimental study of the vibrational spectra of the α, β, and δ phases of octahydro-1,3,5,7-tetranitro-1,3,5,7-tetrazocine (HMX), J. Phys. Chem. B 106 (2002) 10594.
[26] www.ccdc.cam.ac.uk/free_services/mercury/../Mercury_2.3.
[27] W. Smith, I.T. Todorov, A short description of DL_POLY, Mol. Simul. 32 (2006) 935.
[28] S. Nose, A unified formulation of the constant temperature molecular dynamics methods, J. Chem. Phys. 81 (1984) 511.
[29] W.G. Hoover, Canonical dynamics: equilibrium phase-space distributions, Phys. Rev. A 31 (1985) 1695.
[30] M.P. Allen, D.J. Tildesley, Computer Simulation of Liquids, Oxford Science Publications, Oxford, 1987.
[31] R.W. Hockney, J.W. Eastwood, Computer Simulations Using Particles, McGraw-Hill, New York, 1981.
[32] J.M. Rosen, C. Dickinson, Vapor pressures and heats of sublimation of some high-melting organic explosives, J. Chem. Eng. Data 14 (1969) 120.
[33] J.W. Taylor, R.J. Crookes, Vapour pressure and enthalpy of sublimation of 1,3,5,7-tetranitro-1,3,5,7-tetra-azacyclo-octane (HMX), J. Chem. Soc., Faraday Trans. 72 (1976) 723.